Persistent Quantum Beats and Long-Distance Entanglement from Waveguide-Mediated Interactions

Huaixiu Zheng* and Harold U. Baranger†

Department of Physics, Duke University, P.O. Box 90305, Durham, North Carolina 27708, USA

(Received 21 June 2012; published 12 March 2013)

We study photon-photon correlations and entanglement generation in a one-dimensional waveguide coupled to two qubits with an arbitrary spatial separation. To treat the combination of nonlinear elements and 1D continuum, we develop a novel Green function method. The vacuum-mediated qubit-qubit interactions cause quantum beats to appear in the second-order correlation function. We go beyond the Markovian regime and observe that such quantum beats persist much longer than the qubit lifetime. A high degree of long-distance entanglement can be generated, increasing the potential of waveguide-QED systems for scalable quantum networking.

DOI: 10.1103/PhysRevLett.110.113601 PACS numbers: 42.50.Ex, 03.67.Bg, 42.50.Ct, 42.79.Gn

One-dimensional (1D) waveguide-QED systems are emerging as promising candidates for quantum information processing [1–14], motivated by tremendous experimental progress in a wide variety of systems [15–24]. Over the past few years, a *single* emitter strongly coupled to a 1D waveguide has been studied extensively [2–8,10,12–14]. To enable greater quantum networking potential using waveguide QED [1], it is important to study systems having more than just one qubit.

In this Letter, we study cooperative effects of *two* qubits strongly coupled to a 1D waveguide, finding the photon-photon correlations and qubit entanglement beyond the well-studied Markovian regime [25–28]. A key feature is the combination of these two highly nonlinear quantum elements with the 1D continuum of states. In comparison to either linear elements coupled to a waveguide [29–32] or two qubits coupled to a single mode serving as a bus [33], both of which have been studied previously, new physical effects appear. To study these effects, we develop a numerical Green function method to compute the photon correlation function for an arbitrary interqubit separation.

The strong quantum interference in 1D, in contrast to the three-dimensional case [34], makes the vacuum-mediated qubit-qubit interaction [35] long ranged. We find that quantum beats emerge in the photon-photon correlations and persist to much longer time scales in the non-Markovian regime. We show that such persistent quantum beats arise from quantum interference between emission from two subradiant states. Furthermore, we demonstrate that a high degree of long-distance entanglement can be generated, thus supporting waveguide-QED–based open quantum networks.

Hamiltonian.—As shown in Fig. 1(a), we consider two qubits with transition frequencies ω_1 and ω_2, separation $L = \ell_2 - \ell_1$, and dipole couplings to a 1D waveguide. The Hamiltonian of the system is [36]

$$H = \sum_{j=1,2} \hbar(\omega_j - i\Gamma_j'/2)\sigma_j^+\sigma_j^- + H_{\rm wg} + \sum_{j=1,2}\sum_{\alpha=R,L}\int dx \hbar V_j \delta(x-\ell_j)[a_\alpha^\dagger(x)\sigma_j^- + \text{H.c.}],$$
$$H_{\rm wg} = \int dx \frac{\hbar c}{i}\left[a_R^\dagger(x)\frac{d}{dx}a_R(x) - a_L^\dagger(x)\frac{d}{dx}a_L(x)\right], \quad (1)$$

where $a_{R,L}^\dagger(x)$ is the creation operator for a right- or left-going photon at position x and c is the group velocity of photons. σ_j^+ and σ_j^- are the qubit raising and lowering operators, respectively. An imaginary term in the energy level is included to model the spontaneous emission of the excited states at rate $\Gamma_{1,2}'$ to modes other than the waveguide continuum [38]. The decay rate to the waveguide continuum is given by $\Gamma_j = 2V_j^2/c$. Throughout the

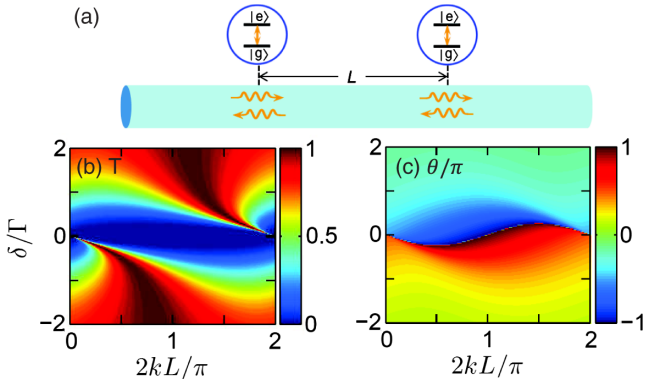

FIG. 1 (color online). Schematic diagram of the waveguide system and single-photon transmission. (a) Two qubits (separated by L) interacting with the waveguide continuum. Panels (b) and (c) show color maps of the single-photon transmission probability T and the phase shift θ, respectively, as a function of detuning $\delta = ck - \omega_0$ and $2kL$. Here, we consider the lossless case $\Gamma' = 0$.

Letter, we assume two identical qubits: $\Gamma_1 = \Gamma_2 \equiv \Gamma$, $\omega_1 = \omega_2 \equiv \omega_0 \gg \Gamma$, and $\Gamma_1' = \Gamma_2' \equiv \Gamma'$.

Single-photon phase gate.—Assuming an incident photon from the left (with wave vector k), we obtain the single-photon scattering eigenstate [39]; the transmission coefficient is given by

$$t_k \equiv \sqrt{T}e^{i\theta} = \frac{(ck - \omega_0 + \frac{i\Gamma'}{2})^2}{(ck - \omega_0 + \frac{i\Gamma + i\Gamma'}{2})^2 + \frac{\Gamma^2}{4}e^{2ikL}}. \quad (2)$$

As shown in Fig. 1(b), there is a large window of perfect transmission: $T \approx 1$, even when the detuning ($\delta = ck - \omega_0$) of the single photon is within the resonance linewidth ($\sim\Gamma$). This is in sharp contrast to the single-qubit case, where perfect transmission is only possible for far off-resonance photons [3]. Such perfect transmission occurs when the reflections from the two qubits interfere destructively and cancel each other completely. Furthermore, Fig. 1(c) shows that within the resonance linewidth, there is a considerable phase shift θ. This feature of single-photon transmission can be used to implement a photon-atom phase gate. For example, in the case of $\delta = -0.5\Gamma$ and $kL = \pi/4$, the single photon passes through the system with unit probability and a $\pi/2$ phase shift. Two successive passes will give rise to a photon-atom π-phase gate, which can be further used to realize a photon-photon phase gate [40].

Photon-photon correlation: Nonlinear effects.—To study the interaction effects, we develop a novel Green function method to calculate the full interacting scattering eigenstates and so photon-photon correlations. We start with a reformulated Hamiltonian [6]

$$H = H_0 + V, \quad V = \sum_{j=1,2} \frac{U}{2} d_j^\dagger d_j (d_j^\dagger d_j - 1),$$
$$H_0 = \sum_{j=1,2} \hbar(\omega_j - i\Gamma_j'/2) d_j^\dagger d_j + H_{\rm wg}$$
$$+ \sum_{j=1,2} \sum_{\alpha=R,L} \int dx \hbar V_j \delta(x - a_j)[a_\alpha^\dagger(x) d_j + \text{H.c.}], \quad (3)$$

where $d_j^\dagger$ and d_j are bosonic creation and annihilation operators on the qubit sites. The qubit ground and excited states correspond to zero- and one-boson states, respectively. Unphysical multiple occupation is removed by including a large repulsive on-site interaction term U; the Hamiltonians in Eqs. (1) and (3) become equivalent in the limit $U \to \infty$. The noninteracting scattering eigenstates can be obtained easily from $H_0|\phi\rangle = E|\phi\rangle$. The full interacting scattering eigenstates $|\psi\rangle$ are connected to $|\phi\rangle$ through the Lippmann-Schwinger equation [11,41,42]

$$|\psi\rangle = |\phi\rangle + G^R(E)V|\psi\rangle, \quad G^R(E) = \frac{1}{E - H_0 + i0^+}. \quad (4)$$

The key step is to numerically evaluate the Green functions, from which one obtains the scattering eigenstates [39]. Assuming a weak continuous wave incident laser, we calculate the second-order correlation function $g_2(t)$ [43] for an arbitrary interqubit separation.

Figure 2 shows $g_2(t)$ for both the transmitted and reflected fields when the probe laser is on resonance with the qubit: $k = k_0$ ($k_0 \equiv \omega_0/c$). When the two qubits are colocated [9] ($L = 0$), $g_2(t)$ of the transmitted field shows strong initial bunching followed by antibunching, while $g_2(t)$ of the reflected field shows perfect antibunching at $t = 0$, $g_2(0) = 0$. This behavior is similar to that in the single-qubit case [3,8]. When the two qubits are spatially separated by $L = \pi/2k_0$, we observe quantum beats (oscillations). Since these beats occur in $g_2(t)$, they necessarily involve the nonlinearity of the qubits and do not occur for, e.g., waveguide-coupled oscillators.

As one increases the separation L, one may expect from the well-known 3D result that the quantum beats disappear [44]. However, in our 1D system they do not: Fig. 3 shows $g_2(t)$ for two cases, $k_0L = 25.5\pi$ and 100.5π, from which it is clear that the beats persist to long time. The 1D nature is key in producing strong quantum interference effects and so long-range qubit-qubit interactions.

Non-Markovian regime.—To interpret these exact numerical results, we compare them with the solution under the well-known Markov approximation. For small separations ($k_0L \leq \pi$), the system is Markovian [44]: The causal propagation time of photons between the two qubits can be neglected, and so the qubits interact instantaneously. To understand quantum beats in this limit, we use a master equation for the density matrix ρ of the qubits in the Markov approximation. Integrating out the 1D bosonic degrees of freedom yields [34]

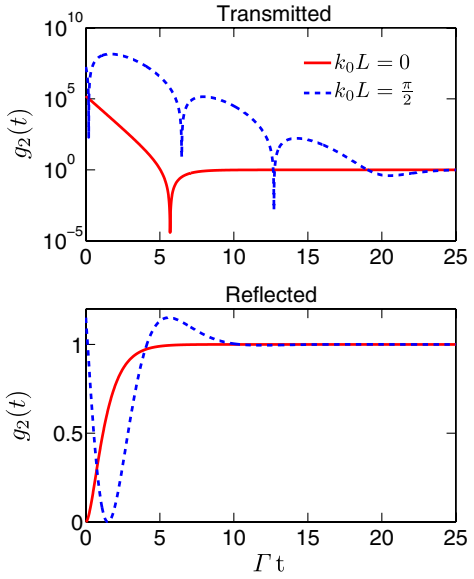

FIG. 2 (color online). Quantum beats in the Markovian regime. The second-order photon-photon correlation function of both the transmitted (top) and reflected (bottom) fields as a function of t for $k_0L = 0$ (solid line) and $k_0L = \pi/2$ (dashed line). The incident weak coherent state is on resonance with the qubits: $k = k_0 = \omega_0/c$. (Parameters: $\omega_0 = 100\Gamma$ and $\Gamma' = 0.1\Gamma$).

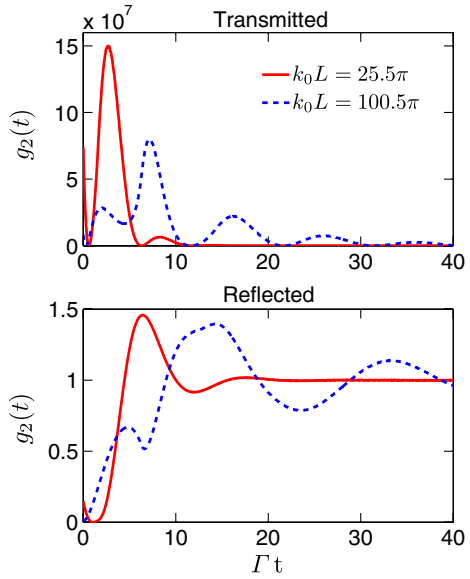

FIG. 3 (color online). Persistent quantum beats in the non-Markovian regime. The second-order correlation function of both the transmitted (top) and reflected (bottom) fields is plotted as a function of t for $k_0L = 25.5\pi$ (solid line) and 100.5π (dashed line). We set the incident coherent state on resonance with the qubits ($k = k_0$), $\omega_0 = 100\Gamma$ and $\Gamma' = 0.1\Gamma$.

$$\frac{\partial\rho}{\partial t} = \frac{i}{\hbar}[\rho, H_c] - \sum_{i,j=1,2} \frac{\Gamma_{ij}}{2}(\rho\sigma_i^+\sigma_j^- + \sigma_i^+\sigma_j^-\rho - 2\sigma_i^-\rho\sigma_j^+),$$
$$H_c = \hbar\omega_0 \sum_{i=1,2} \sigma_i^+\sigma_i^- + \hbar\Omega_{12}(\sigma_1^+\sigma_2^- + \sigma_2^+\sigma_1^-), \quad (5)$$

where $\Gamma_{ii} \equiv \Gamma + \Gamma'$ while $\Gamma_{12} \equiv \Gamma\cos(\omega_0 L/c)$ and $\Omega_{12} \equiv (\Gamma/2)\sin(\omega_0 L/c)$ are the vacuum-mediated spontaneous and coherent couplings, respectively. Transforming to symmetric and antisymmetric states $|S, A\rangle = (|g_1e_2\rangle \pm |e_1g_2\rangle)/\sqrt{2}$ gives a more transparent form:

$$\frac{\partial\rho}{\partial t} = \frac{i}{\hbar}[\rho, H_c] - \sum_{\beta=S,A} \frac{\Gamma_\beta}{2}(\rho\sigma_\beta^+\sigma_\beta^- + \sigma_\beta^+\sigma_\beta^-\rho - 2\sigma_\beta^-\rho\sigma_\beta^+),$$
$$H_c = \sum_{\beta=S,A} \hbar\omega_\beta\sigma_\beta^+\sigma_\beta^-, \quad (6)$$

where $\sigma_{S,A}^+ \equiv (\sigma_1^+ \pm \sigma_2^+)/\sqrt{2}$, $\Gamma_{S,A} \equiv \Gamma + \Gamma' \pm \Gamma_{12}$, and $\omega_{S,A} \equiv \omega_0 \pm \Omega_{12}$. Note that $|S\rangle$ and $|A\rangle$ are decoupled from each other and have transition frequencies $\omega_{S,A}$ and decay rates $\Gamma_{S,A}$ which oscillate as a function of L. When $L = 0$, $\Gamma_S = 2\Gamma + \Gamma'$ and $\Gamma_A = \Gamma'$. $|S\rangle$ is in the superradiant state, while $|A\rangle$ is subradiant. The waveguide couples only to the superradiant state, and so the photon-photon correlation mimics that for a single qubit. However, when $k_0L = \pi/2$, $\Gamma_S = \Gamma_A = \Gamma + \Gamma'$, $\omega_{S,A} = \omega_0 \pm \Gamma/2$, and the waveguide couples to both $|S\rangle$ and $|A\rangle$. The quantum interference between the transitions $|S\rangle \to |g_1g_2\rangle$ and $|A\rangle \to |g_1g_2\rangle$ gives rise to quantum beats at frequency $\omega_S - \omega_A = \Gamma$, as shown in Fig. 2.

As one increases the separation L and goes beyond the Markovian regime, Eq. (5) is not a valid description of the system because the causal propagation time of photons (or retardation effect) has to be included. Comparing the results in Figs. 2 and 3, we see that quantum beats are *more* visible in the non-Markovian regime in both the transmitted and reflected fields and persist to a much longer time scale, especially for the case $k_0L = 100.5\pi$.

To better understand the persistent quantum beats, we extract the transition frequencies and decay rates of the two-qubit system beyond the Markovian regime. This is achieved by analyzing the poles of the Green function [39] defined in Eq. (4); they are given by

$$F(\omega) = \left[\omega - \omega_0 + \frac{i(\Gamma + \Gamma')}{2}\right]^2 + \frac{\Gamma^2}{4}e^{2i\omega L/c} = 0. \quad (7)$$

In the Markovian regime, one can safely replace ω by ω_0 in the exponent, given that $\omega_0 \gg \Gamma$ and $L \ll c\Gamma^{-1}$. Equation (7) then yields $\omega_\pm = \omega_0 - i(\Gamma + \Gamma')/2 \pm i\Gamma e^{i\omega_0 L/c}/2$. The real and imaginary parts of $\omega_\pm$ correspond to the transition frequencies and decay rates, which are nothing but $\omega_{S,A}$ and $-\Gamma_{S,A}/2$ obtained by using the Markov approximation [Eq. (6)]. Beyond this Markovian regime, we solve Eq. (7) iteratively by gradually increasing L.

Figure 4 shows that both $\omega_{S,A}$ and $\Gamma_{S,A}$ deviate significantly from their Markovian values as k_0L becomes large [Figs. 4(c) and 4(d)]. The expanded detail plots Figs. 4(a) and 4(e) show that the Markov approximation works well for $k_0L \in [0, 5\pi]$. At large k_0L, however, *both* the symmetric and antisymmetric states become subradiant [$\Gamma_{S,A} \ll \Gamma$; Fig. 4(f)]. This suppression of decay comes about in the following way: After the initial excitation of and emission from the first qubit, it can be reexcited by the pulse reflected from the second qubit. From the excitation probability of the first qubit over many emission-reexcitation cycles, an effective qubit lifetime can be defined: It is greatly lengthened by the causal propagation of photons between the two qubits. $\Gamma_{S,A}$ characterize the average long time decay quantitatively.

The nonlinear equation (7) gives rise, of course, to infinitely many poles for $L > 0$. These poles represent collective states of two spatially separated qubits with vacuum-mediated interactions. They are eigenmodes of the density matrix of the two qubits. The "two-pole" approximation of retaining only the symmetric and antisymmetric states is a good approximation, because ($\omega_{S,A} - \omega_0$, $\Gamma_{S,A}$) are the two poles closest to the origin (0, 0). Within the parameter range we consider, all other collective states are far detuned from ω_0 and hence barely populated [39]. In addition, $|S\rangle$ and $|A\rangle$ have much smaller decay rates than all the other collective states. Therefore, these two slowly decaying states dominate the long-time dynamics, and quantum interference between their spontaneous emissions is the physical origin of the persistent quantum beats observed in Fig. 3.

Qubit-qubit entanglement.—With the two-pole approximation, we study qubit-qubit entanglement by using the master equation (6) with $\omega_{S,A}$ and $\Gamma_{S,A}$ replaced by the

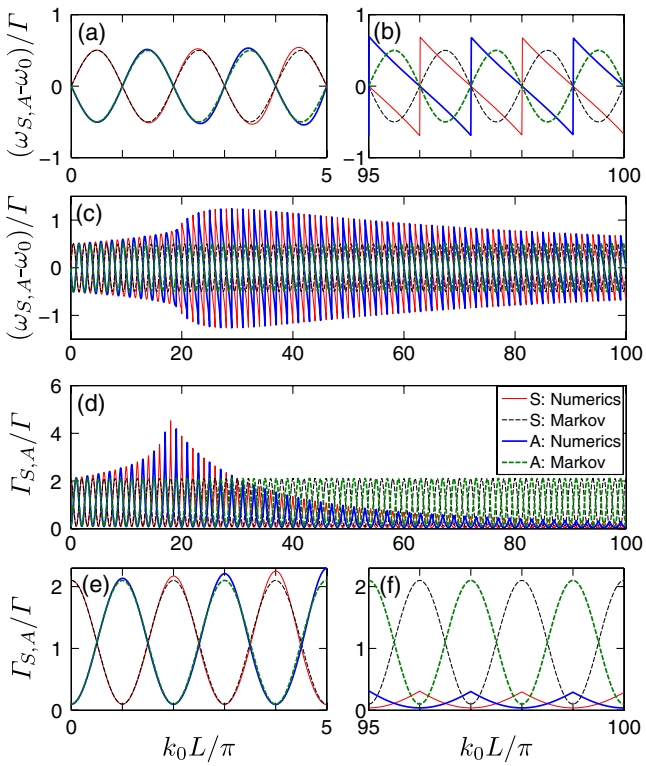

FIG. 4 (color online). Renormalized transition frequencies and decay rates of the symmetric (S) and antisymmetric (A) states. Panels (a)–(c) show the transition frequencies ω_S (thin solid line) and ω_A (thick solid line) obtained numerically from Eq. (7) together with ω_S (thin dashed line) and ω_A (thick dashed line) given by the Markov approximation. Panels (d)–(f) similarly show the decay rates Γ_S and Γ_A obtained both numerically and in the Markov approximation. ($\omega_0 = 100\Gamma$ and $\Gamma' = 0.1\Gamma$).

renormalized values obtained from Eq. (7). We focus on the steady state case by including a continuous weak driving laser on resonance with the first qubit: $H_L = \hbar\Omega_1(\sigma_1^+ + \sigma_1^-)$ [27,28]. The entanglement is characterized by the concurrence [45]; Fig. 5 shows its steady state value for the Rabi frequency $\Omega_1 = 0.1\Gamma$. For small separation [Fig. 5(a)], the concurrence agrees with that obtained by using the Markov approximation [27]: C reaches its maximum when the maximally entangled two-qubit subradiant state (either $|S\rangle$ or $|A\rangle$) has a minimal decay rate and is well populated [28]. Between two peaks, C vanishes, because the symmetric and antisymmetric states are now barely populated and the usual decay rate $\Gamma + \Gamma' \gg \Omega_1$ holds [46].

In contrast, Fig. 5(b) shows that the Markovian predictions break down: We observe enhanced entanglement for an arbitrary interqubit separation. Such enhancement is due to non-Markovian processes: Both $|S\rangle$ and $|A\rangle$ become subradiant (Fig. 4) with decay rates much smaller than Γ and hence are well populated [39]. Thus, long-range entanglement is possible due to non-Markovian processes, making 1D waveguide-QED systems promising candidates for scalable quantum networking.

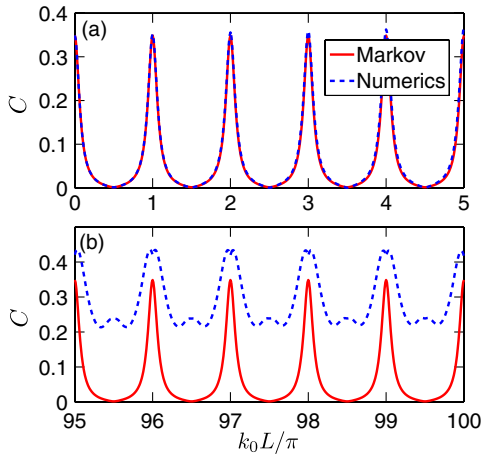

FIG. 5 (color online). Long-distance qubit-qubit entanglement. The steady state concurrence is plotted as a function of k_0L for (a) $0 \le k_0L \le 5\pi$ and (b) $95\pi \le k_0L \le 100\pi$. The Rabi frequencies are $\Omega_1 = 0.1\Gamma$ and $\Omega_2 = 0$. The driving laser is on resonance with the qubits. ($\omega_0 = 100\Gamma$ and $\Gamma' = 0.1\Gamma$).

Discussion of loss.—Accessing the non-Markovian regime requires a large (effective) distance between the qubits and hence low loss in the waveguide. Here, we have included the loss of the qubit by using an effective Purcell factor of 10 (i.e., ~10% loss). Because waveguide loss has the same effect on system performance as qubit loss (both lead to photon leakage), we expect that the observed persistent quantum beats and long-distance entanglement are robust against waveguide loss on this same level, namely, ~10%. While some waveguides in current experimental systems are very lossy (such as plasmonic nanowires [15]), we can circumvent this difficulty by using a hybrid nanofiber system as discussed in the Supplemental Material [39]. One example is an integrated fiber-plasmonic system [3]: The optical fiber is coupled to two tapered plasmonic nanowires which interact with local qubits (e.g., quantum dots). Another example is an integrated nanofiber-trapped atomic ensemble [47,48]: An optical fiber is tapered into a nanofiber in two regions where atomic ensembles are trapped by the evanescent field surrounding the nanofibers. In both of these examples, the long waveguide connecting the two qubits is a high quality optical fiber in which the loss is very small over a length of the order of 100 wavelengths.

We thank D. J. Gauthier for valuable discussions. This work was supported by U.S. NSF Grant No. PHY-10-68698. H. Z. is supported by the Fitzpatrick Institute for Photonics at Duke University. We thank the Fondation Nanosciences of Grenoble, France, for its hospitality during completion of this work.

*hz33@duke.edu
†baranger@phy.duke.edu

[1] H. J. Kimble, Nature (London) **453**, 1023 (2008).
[2] D. E. Chang, A. S. Sørensen, P. R. Hemmer, and M. D. Lukin, Phys. Rev. Lett. **97**, 053002 (2006).

[3] D. E. Chang, A. S. Sørensen, E. A. Demler, and M. D. Lukin, Nat. Phys. **3**, 807 (2007).

[4] J.-T. Shen and S. Fan, Phys. Rev. Lett. **98**, 153003 (2007); Phys. Rev. A **76**, 062709 (2007).

[5] L. Zhou, Z. R. Gong, Y.-X. Liu, C. P. Sun, and F. Nori, Phys. Rev. Lett. **101**, 100501 (2008).

[6] P. Longo, P. Schmitteckert, and K. Busch, Phys. Rev. Lett. **104**, 023602 (2010).

[7] D. Witthaut and A. S. Sørensen, New J. Phys. **12**, 043052 (2010).

[8] H. Zheng, D. J. Gauthier, and H. U. Baranger, Phys. Rev. A **82**, 063816 (2010).

[9] E. Rephaeli, S. E. Kocabas, and S. Fan, Phys. Rev. A **84**, 063832 (2011).

[10] D. Roy, Phys. Rev. Lett. **106**, 053601 (2011).

[11] D. Roy, Phys. Rev. A **83**, 043823 (2011).

[12] P. Kolchin, R. F. Oulton, and X. Zhang, Phys. Rev. Lett. **106**, 113601 (2011).

[13] H. Zheng, D. J. Gauthier, and H. U. Baranger, Phys. Rev. Lett. **107**, 223601 (2011); Phys. Rev. A **85**, 043832 (2012).

[14] E. Rephaeli and S. Fan, Phys. Rev. Lett. **108**, 143602 (2012).

[15] A. V. Akimov, A. Mukherjee, C. L. Yu, D. E. Chang, A. S. Zibrov, P. R. Hemmer, H. Park, and M. D. Lukin, Nature (London) **450**, 402 (2007).

[16] M. Bajcsy, S. Hofferberth, V. Balic, T. Peyronel, M. Hafezi, A. S. Zibrov, V. Vuletic, and M. D. Lukin, Phys. Rev. Lett. **102**, 203902 (2009).

[17] T. M. Babinec, B. J. M. Hausmann, M. Khan, Y. Zhang, J. R. Maze, P. R. Hemmer, and M. Lončar, Nat. Nanotechnol. **5**, 195 (2010).

[18] J. Claudon, J. Bleuse, N. S. Malik, M. Bazin, P. Jaffrennou, N. Gregersen, C. Sauvan, P. Lalanne, and J.-M. Gérard, Nat. Photonics **4**, 174 (2010).

[19] O. Astafiev, A. M. Zagoskin, A. A. Abdumalikov, Y. A. Pashkin, T. Yamamoto, K. Inomata, Y. Nakamura, and J. S. Tsai, Science **327**, 840 (2010).

[20] O. V. Astafiev, A. A. Abdumalikov, A. M. Zagoskin, Y. A. Pashkin, Y. Nakamura, and J. S. Tsai, Phys. Rev. Lett. **104**, 183603 (2010).

[21] J. Bleuse, J. Claudon, M. Creasey, N. S. Malik, J.-M. Gérard, I. Maksymov, J.-P. Hugonin, and P. Lalanne, Phys. Rev. Lett. **106**, 103601 (2011).

[22] I.-C. Hoi, C. M. Wilson, G. Johansson, T. Palomaki, B. Peropadre, and P. Delsing, Phys. Rev. Lett. **107**, 073601 (2011).

[23] A. Laucht, S. Pütz, T. Günthner, N. Hauke, R. Saive, S. Frédérick, M. Bichler, M.-C. Amann, A. W. Holleitner, M. Kaniber, and J. J. Finley, Phys. Rev. X **2**, 011014 (2012).

[24] I.-C. Hoi, T. Palomaki, J. Lindkvist, G. Johansson, P. Delsing, and C. M. Wilson, Phys. Rev. Lett. **108**, 263601 (2012).

[25] D. Dzsotjan, A. S. Sørensen, and M. Fleischhauer, Phys. Rev. B **82**, 075427 (2010).

[26] D. Dzsotjan, J. Kästel, and M. Fleischhauer, Phys. Rev. B **84**, 075419 (2011).

[27] A. Gonzalez-Tudela, D. Martin-Cano, E. Moreno, L. Martin-Moreno, C. Tejedor, and F. J. Garcia-Vidal, Phys. Rev. Lett. **106**, 020501 (2011).

[28] D. Martin-Cano, A. Gonzalez-Tudela, L. Martin-Moreno, F. J. Garcia-Vidal, C. Tejedor, and E. Moreno, Phys. Rev. B **84**, 235306 (2011).

[29] J. P. Paz and A. J. Roncaglia, Phys. Rev. Lett. **100**, 220401 (2008).

[30] T. Zell, F. Queisser, and R. Klesse, Phys. Rev. Lett. **102**, 160501 (2009).

[31] H.-T. Tan, W.-M. Zhang, and G.-x. Li, Phys. Rev. A **83**, 062310 (2011).

[32] A. Wolf, G. D. Chiara, E. Kajari, E. Lutz, and G. Morigi, Europhys. Lett. **95**, 60 008 (2011).

[33] J. Majer, J. M. Chow, J. M. Gambetta, J. Koch, B. R. Johnson, J. A. Schreier, L. Frunzio, D. I. Schuster, A. A. Houck, A. Wallraff, A. Blais, M. H. Devoret, S. M. Girvin, and R. J. Schoelkopf, Nature (London) **449**, 443 (2007).

[34] Z. Ficek and R. Tanas, Phys. Rep. **372**, 369 (2002).

[35] S. Das, G. S. Agarwal, and M. O. Scully, Phys. Rev. Lett. **101**, 153601 (2008).

[36] Note that we adopt the rotating wave approximation at the level of Hamiltonian. As pointed out in Ref. [37], within the rotating wave approximation causality in photon propagation is preserved by extending the frequency integrals to minus infinity. We carry out this scheme in all of our numerical calculations.

[37] P. W. Milonni, D. F. V. James, and H. Fearn, Phys. Rev. A **52**, 1525 (1995).

[38] H. J. Carmichael, *An Open Systems Approach to Quantum Optics* Lect. Notes Phys. (Springer, Berlin, 1993).

[39] See Supplemental Material at http://link.aps.org/supplemental/10.1103/PhysRevLett.110.113601 for details about calculation of single-photon scattering eigenstates, numerical Green function method, the two pole approximation, and possible low-loss experimental systems for long-distance entanglement.

[40] L.-M. Duan and H. J. Kimble, Phys. Rev. Lett. **92**, 127902 (2004).

[41] J. J. Sakurai, *Modern Quantum Mechanics* (Addison-Wesley, Reading, MA, 1994).

[42] A. Dhar, D. Sen, and D. Roy, Phys. Rev. Lett. **101**, 066805 (2008).

[43] R. Loudon, *The Quantum Theory of Light* (Oxford University, New York, 2003), 3rd ed.

[44] Z. Ficek and B. C. Sanders, Phys. Rev. A **41**, 359 (1990).

[45] W. K. Wootters, Phys. Rev. Lett. **80**, 2245 (1998).

[46] The population of an excited state with detuning Δ, decay rate Γ, and Rabi frequency Ω is given by $1/[2 + (\Delta/\Omega)^2 + (\Gamma/2\Omega)^2]$.

[47] E. Vetsch, D. Reitz, G. Sagué, R. Schmidt, S. T. Dawkins, and A. Rauschenbeutel, Phys. Rev. Lett. **104**, 203603 (2010).

[48] A. Goban, K. S. Choi, D. J. Alton, D. Ding, C. Lacroûte, M. Pototschnig, T. Thiele, N. P. Stern, and H. J. Kimble, Phys. Rev. Lett. **109**, 033603 (2012).